J Inf Process Syst, Vol.13, No.3, pp.630~642, June 2017
https://doi.org/10.3745/JIPS.03.0076

ISSN 1976-913X (Print)
ISSN 2092-805X (Electronic)

JOURNAL OF INFORMATION PROCESSING SYSTEMS JIPS

Achievable Rate Analysis for Opportunistic Non-orthogonal Multiple Access-Based Cooperative Relaying Systems

In-Ho Lee* and Howon Lee*

Abstract

In this paper, we propose the opportunistic non-orthogonal multiple access (NOMA)-based cooperative relaying system (CRS) with channel state information (CSI) available at the source, where CSI for the source-to-destination and source-to-relay links is used for opportunistic transmission. Using the CSI, for opportunistic transmission, the source instantaneously chooses between the direct transmission and the cooperative NOMA transmission. We provide an asymptotic expression for the average achievable rate of the opportunistic NOMA-based CRS under Rayleigh fading channels. We verify the asymptotic analysis through Monte Carlo simulations, and compare the average achievable rates of the opportunistic NOMA-based CRS and the conventional one for various channel powers and power allocation coefficients used for NOMA.

Keywords

Achievable Rate Analysis, Decode-and-Forward Relaying, Non-orthogonal Multiple Access, Opportunistic Transmission, Rayleigh Fading Channels, Superposition Coding

1. Introduction

Non-orthogonal multiple access (NOMA) is one of promising techniques to improve the spectral efficiency of wireless multi-user systems [1]. The NOMA scheme uses the power domain for multiple access, and can be implemented by the superposition coding that enables the transmitter to send data signals with different powers to associated different receivers at the same time and bandwidth [2]. In order to enhance the spectral efficiency of cooperative relaying systems (CRSs), the NOMA scheme has been introduced into CRSs in which one or more relays help a source transmit the signals to one or more destinations to mitigate the wireless channel effects such as path loss and shadowing. In industry, the NOMA scheme and the cooperative relaying technique have been considered as key techniques for 3rd Generation Partnership Project (3GPP) Long Term Evolution-Advanced (LTE-A) systems [3,4]. Hence, CRSs using the NOMA scheme can be practically realized as one of alternatives to achieve high spectral efficiency in the fifth generation (5G) communication systems.

In many studies, the advanced NOMA schemes for various CRSs have been developed to significantly

Manuscript received February 23, 2017; first revision May 16, 2017; accepted May 30, 2017.
Corresponding Author: Howon Lee (hwlee@hknu.ac.kr)
* Dept. of Electrical, Electronic and Control Engineering and IITC, Hankyong National University, Anseong, Korea ({ihlee, hwlee}@hknu.ac.kr)

improve the spectral efficiency of the CRSs [5-13]. The studies have focused on the models of CRSs with different node constructions (e.g., the number of relays or destinations) and different relaying schemes (e.g., amplify-and-forward or decode-and-forward relaying), and have shown the spectral efficiency gains achieved by their proposed NOMA schemes in terms of average achievable rate and outage probability. It is noted that the node construction and the relaying scheme can be determined by considering the acceptable complexity and overhead of the CRSs. The detailed literature reviews of NOMA-based CRSs are as follows. In [5], CRS using NOMA has been proposed, where the source simultaneously transmits two independent data symbols by superposition coding, and the relay decodes and forwards the symbol with lower received power after performing the successive interference cancellation (SIC). Also, the average achievable rate for the CRS using NOMA has been analyzed, and a suboptimal power allocation scheme for NOMA has been presented. In [6], a novel detection scheme for CRS using NOMA has been proposed to enhance the achievable rate for CRS using NOMA presented in [5], but it requires the more complicated receiver. In [6], the destination jointly decodes two data symbols from the direct and relayed signals with maximal-ratio combining and SIC. In addition, its average achievable rate and the outage probability have been investigated. Unlike [5] and [6] considering a single relay and a single destination, in [7], the more complicated CRS with multiple relays and destinations has been treated, and a cooperative NOMA scheme has been proposed for the CRS, where the receivers (i.e., relays or destinations) with better channel conditions have prior information about the data symbols of other receivers, and the prior information is used to achieve the spatial diversity. In [7], the outage probability and diversity order achieved by the cooperative NOMA scheme have been studied. Unlike [5-7] with decode-and-forward relaying, in [8], a NOMA-based downlink cooperative cellular system with amplify-and-forward relaying has been proposed, where the base station transmits data signals to two users simultaneously with amplify-and-forward relaying. Also, its average achievable rate and outage performance have been investigated. In [9], the NOMA scheme has been introduced in coordinated direct and relay transmission (CDRT), where the base station directly communicates with a near user while communicating with a far user only through a relay. In the CDRT using NOMA, the near user has the prior information about the data symbol of the far user, and exploits it for interference cancellation, which can significantly improve the spectral efficiency. Its average achievable rate and outage probability have been also analyzed in [9]. In [10], the full-duplex (FD) CRS using NOMA with dual users has been proposed and its average achievable rate and outage probability have been investigated under the assumption of imperfect self-interference cancellation. In addition, it has been shown that the FD CRS using NOMA can work better than the half-duplex CRS using NOMA. In the studies on CRSs using NOMA in [5-10], channel state information (CSI) has been assumed to be unavailable at the source in order to reduce the system overhead. However, it can limit the performance improvement because the source cannot use the time-varying channels for data transmission. In [11-13], hence, adaptive transmission, user selection, and hybrid relaying schemes using CSI have been respectively proposed to enhance the spectral efficiency of CRSs using NOMA.

Unlike the proposed schemes in [11-13], in this paper, we propose the opportunistic NOMA-based CRS using CSI that is available at the source in order to achieve the further performance improvement at the expense of system overhead. In the proposed NOMA-based CRS, we consider a source, a decode-and-forward relay, and a destination to focus on the low complicated CRS for the simple implementation as in [5], where it is noted that advanced NOMA schemes for more complicated CRSs can be studied by using the work presented in this paper. In the proposed NOMA-based CRS, CSI for

the source-to-destination and source-to-relay links is exploited for opportunistic transmission. Based on the CSI, for opportunistic transmission, the source instantaneously selects one of the direct transmission (from the source to the destination) and the cooperative NOMA transmission [5] with the help of the relay, which can provide better achievable rate performance than the conventional NOMA-based CRS with no CSI at the source. In addition, we provide an asymptotic expression for the average achievable rate of the opportunistic NOMA-based CRS assuming Rayleigh fading channels. The asymptotic analysis is verified with Monte Carlo simulations, and the average achievable rates of the opportunistic NOMA-based CRS and the conventional one are compared for different channel powers and power allocation coefficients used for NOMA.

This paper is organized as follows: Section 2 proposes opportunistic NOMA-based CRS, and provides its received signals and signal-to-noise ratios (SNRs). In Section 3, we analyze the average achievable rate for the proposed NOMA-based CRS. In Section 4, we compare the proposed and conventional NOMA-based CRS in terms of the average achievable rate. Section 5 concludes this paper.

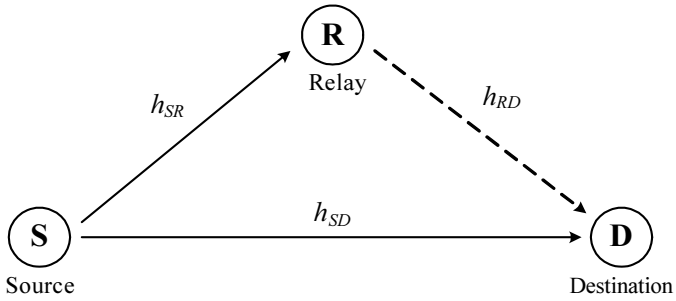

Fig. 1. A cooperative relaying system, where the solid and dashed lines represent the signal transmissions for the first and the second time slots, respectively.

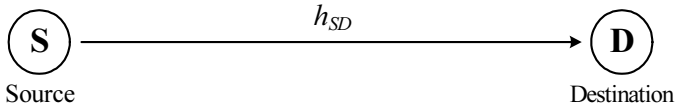

Fig. 2. Direct signal transmission from the source to the destination for a time slot.

2. System Description

We consider the CRS as shown in Fig. 1, where a source (S) transmits signals to a destination (D) directly and through a relay (R). The channel coefficients of S-to-D, S-to-R, and R-to-D links are denoted as h_{SD}, h_{SR}, and h_{RD}, respectively, and assumed to be independent Rayleigh random variables with average powers of β_{SD}, β_{SR}, and β_{RD}, respectively.

In the CRS using NOMA, the source transmits $\sqrt{a_1 P_t}s_1 + \sqrt{a_2 P_t}s_2$ to the relay and the destination during the first time slot, according to the NOMA scheme using the superposition coding [1,5,6], where s_i denotes the i-th data symbol, $\mathrm{E}[|s_i|^2] = 1$, and P_t is the total transmit power. a_i is the power allocation coefficient for symbol s_i, and it is assumed that $a_1 + a_2 = 1$ and $a_1 > a_2$, which means $0.5 < a_1 < 1$ and $0 < a_2 < 0.5$. The relay decodes symbol s_2 after decoding and cancelling symbol s_1

with SIC, whereas the destination decodes symbol s_1 treating symbol s_2 as noise. During the second time slot, then only the relay transmits the decoded symbol s_2 with power P_t to the destination. However, when $|h_{SD}|^2 > |h_{SR}|^2$, the NOMA scheme may not provide a gain of end-to-end achievable rate since the received signal power of symbol s_2 at the relay is very limited. Thus, in this paper, we propose an opportunistic CRS using NOMA (O-NOMA), where if $|h_{SD}|^2 > |h_{SR}|^2$, only direct transmission between the source and the destination is performed without the help of the relay as shown in Fig. 2, otherwise the NOMA scheme is employed with the relay. The rationale of the O-NOMA is based on the fact that the achievable rate for the relayed link is the minimum of achievable rates for the source-to-relay link and the relay-to-destination link. That is, when $|h_{SD}|^2 > |h_{SR}|^2$, the direct link achieves better rate performance than the relayed link. In the O-NOMA, hence, the source directly transmits symbol s_1 to the destination with power P_t during a time slot when $|h_{SD}|^2 > |h_{SR}|^2$.

In the CRS using NOMA, the received signals at the relay and the destination during the first time slot are respectively given as

$$r_{SR}^{C} = h_{SR}\left(\sqrt{a_1 P_t}s_1 + \sqrt{a_2 P_t}s_2\right) + n_{SR}, \tag{1}$$

and

$$r_{SD}^{C} = h_{SD}\left(\sqrt{a_1 P_t}s_1 + \sqrt{a_2 P_t}s_2\right) + n_{SD}, \tag{2}$$

where n_{SR} and n_{SD} denote additive white Gaussian noise with variance σ^2. The received SNRs of symbol s_1 to be decoded for SIC and symbol s_2 to be decoded after SIC at the relay are respectively given from (1) as

$$\gamma_{SR,s_1}^{C} = \frac{|h_{SR}|^2 a_1 P_t}{|h_{SR}|^2 a_2 P_t + \sigma^2}, \tag{3}$$

and

$$\gamma_{SR,s_2}^{C} = \frac{|h_{SR}|^2 a_2 P_t}{\sigma^2}. \tag{4}$$

The received SNR of symbol s_1 to be decoded at the destination is given from (2) as

$$\gamma_{SD,s_1}^{C} = \frac{|h_{SD}|^2 a_1 P_t}{|h_{SD}|^2 a_2 P_t + \sigma^2}. \tag{5}$$

The received signal at the destination during the second time slot is given as

$$r_{RD}^{C} = h_{RD}\sqrt{P_t}s_2 + n_{RD}, \tag{6}$$

where n_{RD} is additive white Gaussian noise with variance σ^2, and thus the received SNR for symbol s_2 is given as

$$\gamma_{RD,s_2}^{C} = \frac{|h_{RD}|^2 P_t}{\sigma^2}. \tag{7}$$

On the other hand, for the direct transmission, the received signal of symbol s_1 at the destination and its received SNR are respectively given as

$$r_{SD}^{D} = h_{SD}\sqrt{P_t}s_1 + n_{SR}, \tag{8}$$

and

$$\gamma_{SD,s_1}^{D} = \frac{|h_{SD}|^2 P_t}{\sigma^2}. \tag{9}$$

In this paper, it is assumed that the relay and the destination perfectly know which one of $|h_{SD}|^2$ and $|h_{SR}|^2$ is larger. In practice, the relay and the destination may report their channel state information (CSI) to the source, and then the source may transmit one-bit information, indicating which channel is in better condition, to them. Hence, the O-NOMA may require more overhead and complexity than the conventional one. It is noted that there may be alternative CSI feedback schemes with low overhead and complexity since the source needs to know only whether $|h_{SD}|^2 > |h_{SR}|^2$ or not.

3. Achievable Rate Analysis

Let $g_{SD} \triangleq |h_{SD}|^2$, $g_{SR} \triangleq |h_{SR}|^2$, $g_{RD} \triangleq |h_{RD}|^2$, $\rho \triangleq P_t/\sigma^2$, and $C(x) \triangleq \log_2(1+x)$, where ρ represents the transmit SNR. Based on the fact that the end-to-end achievable rate of decode-and-forward relaying is dominated by the weakest link [3], and using (3)–(5), (7), and (9), the achievable rate of the O-NOMA is obtained as follows [5]:

If $g_{SD} < g_{SR}$,

$$\begin{aligned} C^{pro} &= \frac{1}{2}\min\left\{\log_2\left(1+\gamma_{SD,s_1}^{C}\right), \log_2\left(1+\gamma_{SR,s_1}^{C}\right)\right\} \\ &\quad + \frac{1}{2}\min\left\{\log_2\left(1+\gamma_{SR,s_2}^{C}\right), \log_2\left(1+\gamma_{RD,s_2}^{C}\right)\right\} \qquad (10) \\ &= \frac{1}{2}\log_2\left(1+\gamma_{SD,s_1}^{C}\right) \\ &\quad + \frac{1}{2}\min\left\{\log_2\left(1+\gamma_{SR,s_2}^{C}\right), \log_2\left(1+\gamma_{RD,s_2}^{C}\right)\right\}. \qquad (11) \end{aligned}$$

Otherwise,

$$C^{pro} = \log_2\left(1+\gamma_{SD,s_1}^{D}\right). \tag{12}$$

In (10), it is noted that the first and the second parts denote the achievable rates of symbols s_1 and s_2, respectively. In the first part of (10), $\log_2\left(1+\gamma_{SR,s_1}^{C}\right)$ is required to assume that the relay successfully decodes symbol s_1 for SIC, but that is deleted in (11) since $g_{SD} < g_{SR}$. It is also noted that there is one half spectral efficiency penalty for relaying in (11), whereas there is no spectral efficiency penalty in (12) as the source transmits an independent data symbol to the destination directly for a given time slot when $g_{SD} > g_{SR}$. Then, using (11) and (12), the achievable average rate of the O-NOMA is obtained as

$$\bar{C}^{pro} = \int_0^\infty \int_0^\infty \int_y^\infty C(x\rho) f_{g_{SD}}(x) f_{g_{SR}}(y) f_{g_{RD}}(z)\, dx\, dy\, dz + \int_0^\infty \int_0^\infty \int_0^y \left[\frac{1}{2} C\left(\frac{x a_1 \rho}{x a_2 \rho + 1}\right) + \frac{1}{2}\min\{C(y a_2 \rho), C(z\rho)\}\right] \times f_{g_{SD}}(x) f_{g_{SR}}(y) f_{g_{RD}}(z)\, dx\, dy\, dz, \quad (13)$$

where $f_X(\cdot)$ denotes the probability density function (PDF) of random variable X, and $f_{g_\delta}(x) = (1/\beta_\delta) e^{-x/\beta_\delta}$ for $\delta \in \{SD, SR, RD\}$. Since mathematical analysis of (13) is intractable, we focus on asymptotic rate analysis using high SNR approximation. Applying high SNR approximation to (13), the average rate is then approximated as follows:

$$\bar{C}^{pro} \approx \underbrace{\int_0^\infty \int_0^\infty \int_y^\infty C(x\rho) f_{g_{SD}}(x) f_{g_{SR}}(y) f_{g_{RD}}(z)\, dx\, dy\, dz}_{\triangleq \Psi_1} + \underbrace{\int_0^\infty \int_0^\infty \int_0^y \frac{1}{2} C\left(\frac{a_1}{a_2}\right) f_{g_{SD}}(x) f_{g_{SR}}(y) f_{g_{RD}}(z)\, dx\, dy\, dz}_{\triangleq \Psi_2} + \underbrace{\int_0^\infty \int_0^\infty \int_0^y \frac{1}{2}\min\{C(y a_2 \rho), C(z\rho)\} f_{g_{SD}}(x) f_{g_{SR}}(y) f_{g_{RD}}(z)\, dx\, dy\, dz}_{\triangleq \Psi_3}. \quad (14)$$

Ψ_1 in (14) is derived as

$$\begin{aligned}\Psi_1 &= \int_0^\infty \int_0^\infty \int_0^x C(x\rho) f_{g_{SR}}(y) f_{g_{SD}}(x) f_{g_{RD}}(z)\, dy\, dx\, dz \\ &= \int_0^\infty C(x\rho)\left(1 - e^{-x/\beta_{SR}}\right) \frac{1}{\beta_{SD}} e^{-x/\beta_{SD}} dx \\ &= -\log_2 e \left\{ e^{1/(\beta_{SD}\rho)} \mathrm{Ei}\left(-\frac{1}{\beta_{SD}\rho}\right) - \left(\frac{1}{\beta_{SD}} + \frac{1}{\beta_{SR}}\right)^{-1} \times \frac{1}{\beta_{SD}} e^{\frac{1}{\rho}\left(\frac{1}{\beta_{SD}} + \frac{1}{\beta_{SR}}\right)} \mathrm{Ei}\left(-\frac{1}{\rho}\left(\frac{1}{\beta_{SD}} + \frac{1}{\beta_{SR}}\right)\right)\right\}, \end{aligned} \quad (15)$$

where we use $\int_0^\infty e^{-\mu x} \ln(1+\eta x) = -\frac{1}{\mu} e^{\frac{\mu}{\eta}} \mathrm{Ei}(-\mu/\eta)$ in [14, eq. (4.337.2)], and $\mathrm{Ei}(\cdot)$ denotes the exponential integral function in [14, eq. (8.211.1)]. Then, Ψ_2 in (14) is obtained as

$$\begin{aligned}\Psi_2 &= \frac{1}{2} C\left(\frac{a_1}{a_2}\right) \int_0^\infty \int_0^\infty \int_0^y f_{g_{SD}}(x) f_{g_{SR}}(y) f_{g_{RD}}(z)\, dx\, dy\, dz \\ &= \frac{1}{2} C\left(\frac{a_1}{a_2}\right) \left\{ 1 - \int_0^\infty \int_0^\infty \frac{1}{\beta_{SR}} e^{-y\left(\frac{1}{\beta_{SD}} + \frac{1}{\beta_{SR}}\right)} \frac{1}{\beta_{RD}} e^{-\frac{z}{\beta_{RD}}}\, dy\, dz \right\} \\ &= \frac{1}{2} C\left(\frac{a_1}{a_2}\right) \left(\frac{\beta_{SR}}{\beta_{SD} + \beta_{SR}}\right). \end{aligned} \quad (16)$$

Using $\int_0^\infty e^{-\mu x} \ln(1+\eta x) = -\frac{1}{\mu} e^{\frac{\mu}{\eta}} \mathrm{Ei}(-\mu/\eta)$ in [14, eq. (4.337.2)], Ψ_3 in (14) is derived as follows:

$$\begin{aligned}
\Psi_3 &= \int_0^{\infty}\int_0^{z/a_2}\int_0^{y}\frac{1}{2}C(ya_2\rho)f_{g_{SD}}(x)f_{g_{SR}}(y)f_{g_{RD}}(z)\,dx\,dy\,dz \\
&\quad+\int_0^{\infty}\int_{z/a_2}^{\infty}\int_0^{y}\frac{1}{2}C(z\rho)f_{g_{SD}}(x)f_{g_{SR}}(y)f_{g_{RD}}(z)\,dx\,dy\,dz \\
&= \int_0^{\infty}\int_{a_2y}^{\infty}\frac{1}{2}C(ya_2\rho)\left(1-e^{-y/\beta_{SD}}\right)\frac{e^{-\frac{y}{\beta_{SR}}-\frac{z}{\beta_{RD}}}}{\beta_{SR}\beta_{RD}}\,dz\,dy \\
&\quad+\int_0^{\infty}\int_{z/a_2}^{\infty}\frac{1}{2}C(z\rho)\left(1-e^{-y/\beta_{SD}}\right)\frac{e^{-\frac{y}{\beta_{SR}}-\frac{z}{\beta_{RD}}}}{\beta_{SR}\beta_{RD}}\,dy\,dz \\
&= \int_0^{\infty}\frac{1}{2}C(ya_2\rho)\left(1-e^{-y/\beta_{SD}}\right)\frac{e^{-y\left(\frac{1}{\beta_{SR}}+\frac{a_2}{\beta_{RD}}\right)}}{\beta_{SR}}\,dy \\
&\quad+\int_0^{\infty}\frac{1}{2}C(z\rho)\left\{e^{-z/(a_2\beta_{SR})}-\left(\frac{1}{\beta_{SD}}+\frac{1}{\beta_{SR}}\right)^{-1}\frac{e^{-\frac{z}{a_2}\left(\frac{1}{\beta_{SD}}+\frac{1}{\beta_{SR}}\right)}}{\beta_{SR}}\right\}\frac{e^{-\frac{z}{\beta_{RD}}}}{\beta_{RD}}dz \\
&= -\frac{\log_2 e}{2}\left\{\left(\frac{1}{a_2\beta_{SR}}+\frac{1}{\beta_{RD}}\right)^{-1}\frac{e^{\frac{1}{\rho}\left(\frac{1}{a_2\beta_{SR}}+\frac{1}{\beta_{RD}}\right)}}{a_2\beta_{SR}}\mathrm{Ei}\left(-\frac{1}{\rho}\left(\frac{1}{a_2\beta_{SR}}+\frac{1}{\beta_{RD}}\right)\right)\right. \\
&\quad-\left(\frac{1}{a_2\beta_{SD}}+\frac{1}{a_2\beta_{SR}}+\frac{1}{\beta_{RD}}\right)^{-1}\frac{e^{\frac{1}{\rho}\left(\frac{1}{a_2\beta_{SD}}+\frac{1}{a_2\beta_{SR}}+\frac{1}{\beta_{RD}}\right)}}{a_2\beta_{SR}}\mathrm{Ei}\left(-\frac{1}{\rho}\left(\frac{1}{a_2\beta_{SD}}+\frac{1}{a_2\beta_{SR}}+\frac{1}{\beta_{RD}}\right)\right) \\
&\quad+\left(\frac{1}{a_2\beta_{SR}}+\frac{1}{\beta_{RD}}\right)^{-1}\frac{e^{\frac{1}{\rho}\left(\frac{1}{a_2\beta_{SR}}+\frac{1}{\beta_{RD}}\right)}}{\beta_{RD}}\mathrm{Ei}\left(-\frac{1}{\rho}\left(\frac{1}{a_2\beta_{SR}}+\frac{1}{\beta_{RD}}\right)\right) \\
&\quad-\left(\frac{1}{\beta_{SD}}+\frac{1}{\beta_{SR}}\right)^{-1}\left(\frac{1}{a_2\beta_{SD}}+\frac{1}{a_2\beta_{SR}}+\frac{1}{\beta_{RD}}\right)^{-1}\frac{e^{\frac{1}{\rho}\left(\frac{1}{a_2\beta_{SD}}+\frac{1}{a_2\beta_{SR}}+\frac{1}{\beta_{RD}}\right)}}{\beta_{SR}\beta_{RD}} \\
&\quad\left.\times\mathrm{Ei}\left(-\frac{1}{\rho}\left(\frac{1}{a_2\beta_{SD}}+\frac{1}{a_2\beta_{SR}}+\frac{1}{\beta_{RD}}\right)\right)\right\}. \qquad (17)
\end{aligned}$$

Using the approximations of $\mathrm{Ei}(-x)\approx C_E+\ln(x)$ for $x\to 0$ in [14, eq. (8.212.1)] and $e^x\approx 1$ for $x\to 0$, where C_E denotes the Euler constant, (15) and (17) are respectively approximated for $\rho\to\infty$ as follows:

$$\Psi_1 \approx -\log_2 e\left[C_E+\ln\left(\frac{1}{\beta_{SD}\,\rho}\right)-\left(\frac{\beta_{SR}}{\beta_{SD}+\beta_{SR}}\right)\left\{C_E+\ln\left(\frac{1}{\rho}\left(\frac{1}{\beta_{SD}}+\frac{1}{\beta_{SR}}\right)\right)\right\}\right], \qquad (18)$$

and

$$\begin{aligned}
\Psi_3 &\approx -\frac{\log_2 e}{2}\left[\left(\frac{\beta_{RD}}{a_2\beta_{SR}+\beta_{RD}}\right)\left\{C_E+\ln\left(\frac{1}{\rho}\left(\frac{1}{a_2\beta_{SR}}+\frac{1}{\beta_{RD}}\right)\right)\right\}\right. \\
&\quad-\frac{1}{a_2\beta_{SR}}\left(\frac{1}{a_2\beta_{SD}}+\frac{1}{a_2\beta_{SR}}+\frac{1}{\beta_{RD}}\right)^{-1}\left\{C_E+\ln\left(\frac{1}{\rho}\left(\frac{1}{a_2\beta_{SD}}+\frac{1}{a_2\beta_{SR}}+\frac{1}{\beta_{RD}}\right)\right)\right\} \\
&\quad\left.+\left(\frac{a_2\beta_{SR}}{a_2\beta_{SR}+\beta_{RD}}\right)\left\{C_E+\ln\left(\frac{1}{\rho}\left(\frac{1}{a_2\beta_{SR}}+\frac{1}{\beta_{RD}}\right)\right)\right\}\right.
\end{aligned}$$

$$-\frac{1}{\beta_{RD}}\left(\frac{\beta_{SD}}{\beta_{SD}+\beta_{SR}}\right)\left(\frac{1}{a_2\beta_{SD}}+\frac{1}{a_2\beta_{SR}}+\frac{1}{\beta_{RD}}\right)^{-1}$$
$$\times\left\{C_E+\ln\left(\frac{1}{\rho}\left(\frac{1}{a_2\beta_{SD}}+\frac{1}{a_2\beta_{SR}}+\frac{1}{\beta_{RD}}\right)\right)\right\}\Bigg]. \quad (19)$$

Summing (16), (18), and (19), and inserting $a_1 = 1 - a_2$, the asymptotic average rate of the O-NOMA for $\rho \to \infty$ is finally obtained as

$$\bar{C}^{pro} \approx \frac{1}{2}\left(3-\frac{2\beta_{SR}+\beta_{SD}}{\beta_{SD}+\beta_{SR}}\right)(\log_2\rho - C_E\log_2 e)+\frac{1}{2}\left(\frac{\beta_{SR}}{\beta_{SD}+\beta_{SR}}\right)\log_2\left(\frac{1}{a_2}\right)$$
$$+\log_2\beta_{SD}+\left(\frac{\beta_{SR}}{\beta_{SD}+\beta_{SR}}\right)\log_2\left(\frac{1}{\beta_{SD}}+\frac{1}{\beta_{SR}}\right)-\frac{1}{2}\log_2\left(\frac{1}{a_2\beta_{SR}}+\frac{1}{\beta_{RD}}\right)$$
$$+\frac{1}{2}\left(\frac{\beta_{SD}}{\beta_{SD}+\beta_{SR}}\right)\log_2\left(\frac{1}{a_2\beta_{SD}}+\frac{1}{a_2\beta_{SR}}+\frac{1}{\beta_{RD}}\right). \quad (20)$$

4. Numerical Results

For performance comparison, the average rate of the conventional CRS using NOMA (C-NOMA) is considered in this paper. In the C-NOMA, the NOMA scheme presented in Section 2 is always used regardless of the channel conditions. Thus, the achievable rate of the C-NOMA is given as (10), and its asymptotic average rate for $\rho \to \infty$ is given as [5, eq. (15)]

$$\bar{C}^{con} \approx \frac{1}{2}\log_2\rho - \frac{\log_2 e}{2}C_E - \frac{1}{2}\log_2\left(\frac{1}{\beta_{SR}}+\frac{a_2}{\beta_{RD}}\right). \quad (21)$$

In Figs. 3–7, the simulation results for the proposed O-NOMA and the C-NOMA represent their exact average achievable rates obtained by averaging (11) and (12) for O-NOMA and (10) for C-NOMA, respectively, through Monte Carlo simulations. The asymptotic results for the proposed O-NOMA and the C-NOMA denote the analytic results obtained from (20) and (21), respectively.

Figs. 3 and 4 show the average achievable rates for O-NOMA and C-NOMA with various transmit SNR values when $a_1 = 0.9$, $a_2 = 0.1$, and $\beta_{SD} = 1$. In particular, in Fig. 3 their average achievable rates are compared for different average channel powers of the R-to-D link (i.e., $\beta_{RD} = 1$, 10) when $\beta_{SR} = 1$, whereas in Fig. 4 their average achievable rates are compared for different average channel powers of the S-to-R link (i.e., $\beta_{SR} = 1$, 10) when $\beta_{RD} = 1$. From the figures, it is observed that the asymptotic results for the proposed O-NOMA are in perfect agreement with the simulation results in the high transmit SNR regime. Fig. 3 demonstrates that an increase in the average channel power of the R-to-D link does not affect the average rate performances for both O-NOMA and C-NOMA. In addition, the proposed O-NOMA attains better average rate performance than C-NOMA as the transmit SNR goes up. On the other hand, Fig. 4 indicates that the average rate for the proposed O-NOMA becomes worse but that for C-NOMA becomes better as the average channel power of the S-to-R link increases. Thus, a rate gain attainable by O-NOMA over C-NOMA becomes smaller with an increase in the average channel power of the S-to-R link.

Figs. 5–7 show the average achievable rates for O-NOMA and C-NOMA with various power allocation coefficients when $\rho = 20$ dB, 30 dB, and $\beta_{SD} = 1$. Especially, their average achievable rates are compared for $\beta_{SR} = \beta_{RD} = 1$ in Fig. 5, $\beta_{SR} = 1$ and $\beta_{RD} = 10$ in Fig. 6, and $\beta_{SR} = 10$ and $\beta_{RD} = 1$ in Fig. 7, respectively. In the figures, the asymptotic results for O-NOMA perfectly match the simulation results for high transmit SNR (i.e., $\rho = 20$ dB, 30 dB) and $0.1 < a_2 < 0.5$, where it is noted that the asymptotic results for low transmit SNR are not shown in this paper since a considerable difference between the asymptotic and simulated results exists. O-NOMA attains better average rate performance as compared with C-NOMA in a high transmit SNR regime, and hence their performance evaluation for high transmit SNR can be more meaningful. In addition, from the figures, it is illustrated that O-NOMA has better average rate performance than C-NOMA as the transmit SNR rises, which is the same aspect as seen in Figs. 3 and 4. In Figs. 5 and 6, the average rate performances for both O-NOMA and C-NOMA are almost not changed by the power allocation coefficients for $0 < a_2 < 0.5$ when $\beta_{SR} = 1$ and $\beta_{RD} = 1, 10$, where it is noted that $a_1 = 1 - a_2$. However, in Fig. 7 for $\beta_{SR} = 10$ and $\beta_{RD} = 1$, their average rate performances are considerably changed by the power allocation coefficients. From the results, it is recognized that a pertinent power allocation coefficient may be required to improve the average rate for O-NOMA when the average channel power of the S-to-R link is large.

It is noteworthy that O-NOMA achieves better average rate performance than C-NOMA at the expense of CSI feedback or other feedback schemes with lower overhead and complexity to provide the source with the information about which one of the S-to-D and the S-to-R links has better instantaneous channel power.

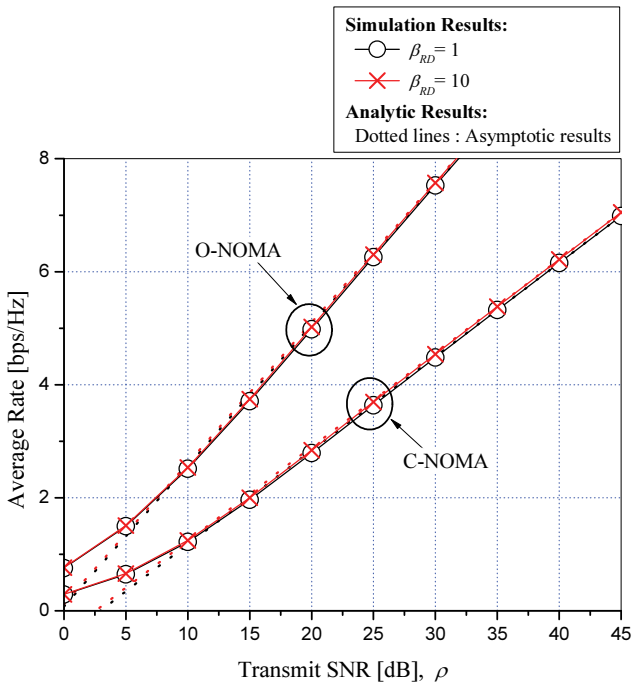

Fig. 3. Average achievable rates of O-NOMA and C-NOMA for $a_1 = 0.9$ and $a_2 = 0.1$ when $\beta_{SD} = \beta_{SR} = 1$ and $\beta_{RD} = 1, 10$.

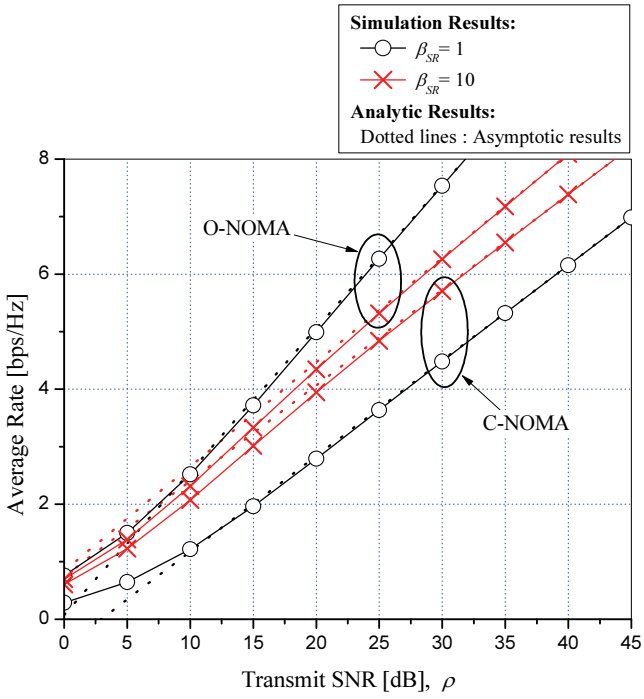

Fig. 4. Average achievable rates of O-NOMA and C-NOMA for $a_1 = 0.9$ and $a_2 = 0.1$ when $\beta_{SD} = \beta_{RD} = 1$ and $\beta_{SR} = 1, 10$.

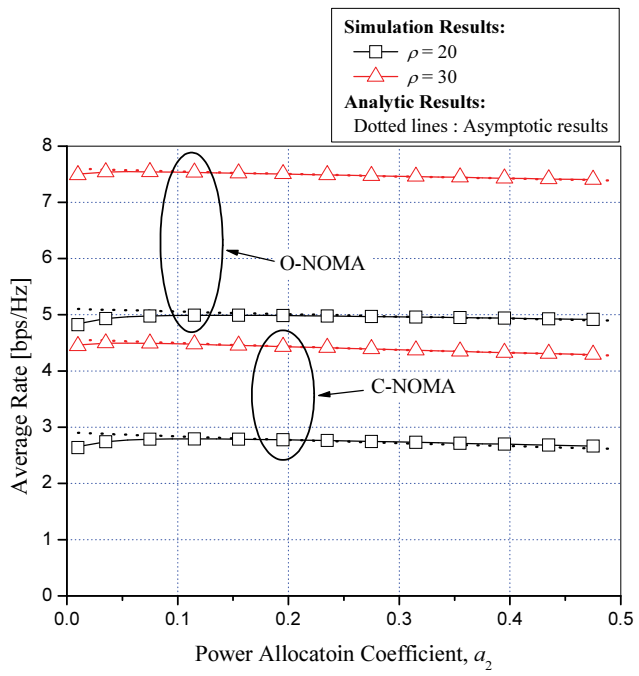

Fig. 5. Average achievable rates of O-NOMA and C-NOMA for $\rho = 20$ dB, 30 dB when $\beta_{SD} = \beta_{SR} = \beta_{RD} = 1$.

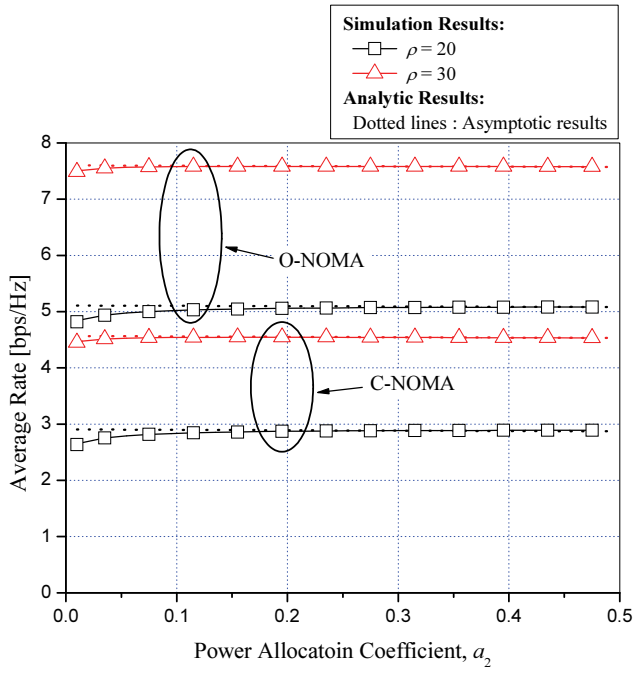

Fig. 6. Average achievable rates of O-NOMA and C-NOMA for $\rho = 20$ dB, 30 dB when $\beta_{SD} = \beta_{SR} = 1$ and $\beta_{RD} = 10$.

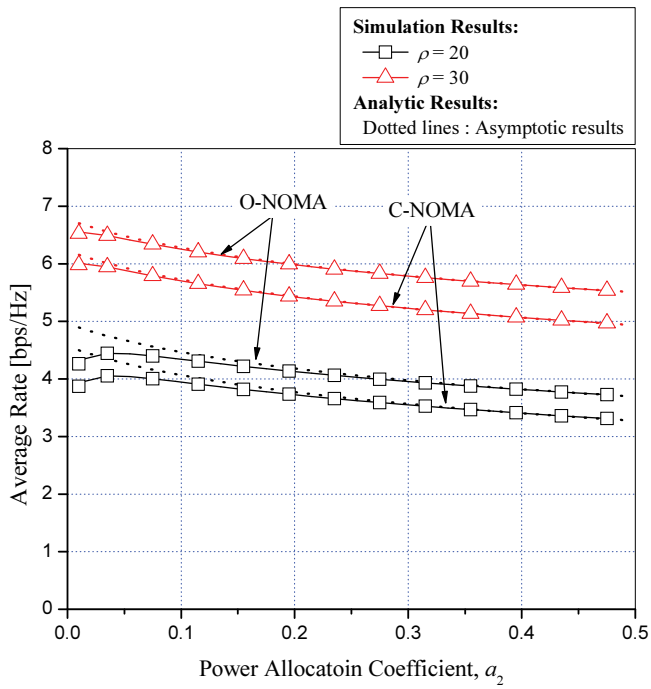

Fig. 7. Average achievable rates of O-NOMA and C-NOMA for $\rho = 20$ dB, 30 dB when $\beta_{SD} = \beta_{RD} = 1$ and $\beta_{SR} = 10$.

5. Conclusions

In this paper, we have proposed the opportunistic NOMA-based CRS using CSI available at the source, and provided an asymptotic expression for the average achievable rate of the opportunistic NOMA-based CRS under Rayleigh fading channels. From the numerical results, we show that the proposed NOMA-based CRS achieves better rate performance than the conventional NOMA-based CRS as the transmit SNR increases. Also, a rate gain achievable by the proposed NOMA-based CRS over the conventional one becomes larger as the average channel power of the S-to-R link decreases. However, the rate gain of the proposed NOMA-based CRS is not affected by the average channel power of the R-to-D link. Furthermore, the average rate performance of the proposed NOMA-based CRS is considerably affected by the power allocation coefficient used for NOMA when the average channel power of the S-to-R link is large. Hence, the proposed NOMA-based CRS can be more beneficial than the conventional one in terms of the achievable rate when the transmit SNR is high, and the average channel power of the S-to-R link is small, but the proposed one requires CSI feedback or alternative feedback schemes with lower overhead and complexity.

Acknowledgement

This work was partly supported by Institute for Information & Communications Technology Promotion (IITP) grant funded by the Korea government (MSIP) (No. 2013-0-00405, Development of Device Collaborative Giga-Level Smart Cloudlet Technology) and the GRRC program of Gyeonggi province (No. GRRC HANKYONG 2012-B02, Development of Vision Inspection algorithm and Wireless and Wired Integrated Control System for Intelligent Logistics Inspection).

References

[1] Z. Ding, Z. Yang, P. Fan, and H. V. Poor, "On the performance of non-orthogonal multiple access in 5G systems with randomly deployed users," *IEEE Signal Processing Letters*, vol. 21, no. 12, pp. 1501-1505, 2014.

[2] H. T. Do and S. Y. Chung, "Linear beamforming and superposition coding with common information for the Gaussian MIMO broadcast channel," *IEEE Transactions on Communications*, vol. 57, no. 8, pp. 2484-2494, 2009.

[3] 3rd Generation Partnership Project (3GPP), "Technical specification group radio access network; study on downlink multiuser superposition transmission (MUST) for LTE (Release 13)," 3GPP Technical Specification Group Radio Access Network, *Technical Report TR 36.859 V13.0.0*, 2015.

[4] 3rd Generation Partnership Project (3GPP), "Evolved universal terrestrial radio access (E-UTRA); physical layer for relaying operation (Release 10)," 3GPP Technical Specification Group Radio Access Network, *Technical Specification TS 36.216 V10.2.0*, 2013.

[5] J. B. Kim and I. H. Lee, "Capacity analysis of cooperative relaying systems using non-orthogonal multiple access," *IEEE Communications Letters*, vol. 19, no. 11, pp. 1949-1952, 2015.

[6] M. Xu, F. Ji, M. Wen, and W. Duan, "Novel receiver design for the cooperative relaying system with non-orthogonal multiple access," *IEEE Communications Letters*, vol. 20, no. 8, pp. 1679-1682, 2016

[7] Z. Ding, M. Peng, and H. V. Poor, "Cooperative non-orthogonal multiple access in 5G systems," *IEEE Communications Letters*, vol. 19, no. 8, pp. 1462-1465, 2015.

[8] J. Men and J. Ge, "Performance analysis of non-orthogonal multiple access in downlink cooperative network," *IET Communications*, vol. 9, no. 18, pp. 2267-2273, 2015.

[9] J. B. Kim and I. H. Lee, "Non-orthogonal multiple access in coordinated direct and relay transmission," *IEEE Communications Letters*, vol. 19, no. 11, pp. 2037-2040, 2015.

[10] C. Zhong and Z. Zhang, "Non-orthogonal multiple access with cooperative full-duplex relaying," *IEEE Communications Letters*, vol. 20, no. 12, pp. 2478-2481, 2016.

[11] S. Luo and K. C. Teh, "Adaptive transmission for cooperative NOMA system with buffer-aided relaying," *IEEE Communications Letters*, vol. 21, no. 4, pp. 937-940, 2017.

[12] N. T. Do, D. B. da Costa, T. Q. Duong, and B. An, "A BNBF user selection scheme for NOMA-based cooperative relaying systems with SWIPT," *IEEE Communications Letters*, vol. 21, no. 3, pp. 664-667, 2017.

[13] Y. Liu, G. Pan, H. Zhang, and M. Song, "Hybrid decode-forward & amplify-forward relaying with non-orthogonal multiple access," *IEEE Access*, vol. 4, pp. 4912-4921, 2016.

[14] I. S. Gradshteyn and I. M. Ryzhik, *Table of Integrals, Series, and Products*, 7th ed. Burlington, MA: Academic Press, 2007.

In-Ho Lee http://orcid.org/0000-0002-2104-9781

He received the B.S., M.S., and Ph.D. degrees in electrical engineering from Hanyang University, Ansan, Korea, in 2003, 2005 and 2008, respectively. He worked for LTE-Advanced standardization in Samsung Electronics Co. from 2008 to 2010. He was a Post-Doctoral Fellow at the Department of Electrical Engineering, Hanyang University, Ansan, Korea, from April 2010 to March 2011. Since March 2011, he has been with the Department of Electrical, Electronic, and Control Engineering, Hankyong National University, Anseong, Korea. His present research interests include non-orthogonal multiple access, millimeter wave wireless communications, cooperative communications, multi-hop relaying, transmission and reception of multiple-input and multiple-output communications, multicast communications, and multi-user channel state information feedback.

Howon Lee http://orcid.org/0000-0001-5509-9202

He is an associate professor in the Department of Electrical, Electronic and Control Engineering (EECE) at Hankyong National University (HKNU). He received his BS, MS, and PhD in electrical engineering from Korea Advanced Institute of Science and Technology (KAIST) in 2003, 2005, and 2009, respectively. Before joining HKNU, he was a team leader of knowledge convergence team at KAIST Institute for Information Technology (IT) Convergence until 2012. His current research interests include knowledge communications, IT convergence, cross-layer radio resource management, cognitive radio, Voice over IP (VoIP) service, wireless communications, compressed sensing, and wireless power transfer. He is also the recipient of the JCCI 2006 Best Paper Award, Intel Student Paper Contest Bronze Prize in 2006 and TTA Paper Contest Encouragement Award in 2011.